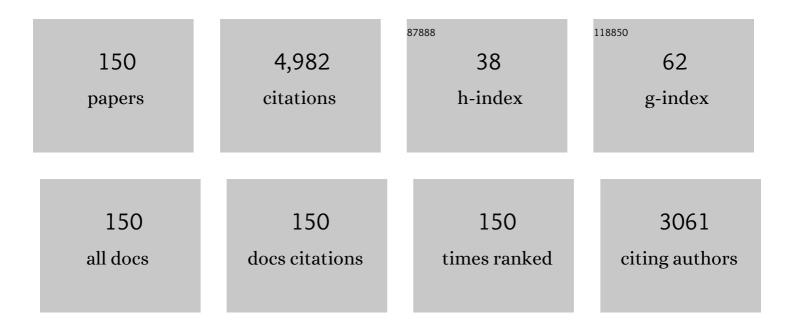
List of Publications by Year in descending order

Source: https://exaly.com/author-pdf/5994605/publications.pdf Version: 2024-02-01



#	Article	IF	CITATIONS
1	Experimental and kinetic modeling study of laminar burning velocities of NH3/air, NH3/H2/air, NH3/N3/N3/CO/air and NH3/CH4/air premixed flames. Combustion and Flame, 2019, 206, 214-226.	5.2	353
2	Simultaneous removal of NOx, SO2 and Hg in nitrogen flow in a narrow reactor by ozone injection: Experimental results. Fuel Processing Technology, 2007, 88, 817-823.	7.2	259
3	Effects of microwave irradiation treatment on physicochemical characteristics of Chinese low-rank coals. Energy Conversion and Management, 2013, 71, 84-91.	9.2	189
4	Experimental study and kinetic analysis of the laminar burning velocity of NH3/syngas/air, NH3/CO/air and NH3/H2/air premixed flames at elevated pressures. Combustion and Flame, 2020, 221, 270-287.	5.2	141
5	Flue gas treatment with ozone oxidation: An overview on NO , organic pollutants, and mercury. Chemical Engineering Journal, 2020, 382, 123030.	12.7	129
6	Up-to-date life cycle assessment and comparison study of clean coal power generation technologies in China. Journal of Cleaner Production, 2013, 39, 24-31.	9.3	123
7	Catalytic deep oxidation of NO by ozone over MnO x loaded spherical alumina catalyst. Applied Catalysis B: Environmental, 2016, 198, 100-111.	20.2	106
8	Comparative investigation on catalytic ozonation of VOCs in different types over supported MnO catalysts. Journal of Hazardous Materials, 2020, 391, 122218.	12.4	106
9	Pyrolysis behavior of a typical Chinese sub-bituminous Zhundong coal from moderate to high temperatures. Fuel, 2016, 185, 701-708.	6.4	100
10	In-situ Measurement of Sodium and Potassium Release during Oxy-Fuel Combustion of Lignite using Laser-Induced Breakdown Spectroscopy: Effects of O ₂ and CO ₂ Concentration. Energy & Fuels, 2013, 27, 1123-1130.	5.1	97
11	Low temperature catalytic ozonation of toluene in flue gas over Mn-based catalysts: Effect of support property and SO2/water vapor addition. Applied Catalysis B: Environmental, 2020, 266, 118662.	20.2	93
12	Influence of the hydrothermal dewatering on the combustion characteristics of Chinese low-rank coals. Applied Thermal Engineering, 2015, 90, 174-181.	6.0	86
13	Investigation of laminar flame speeds of typical syngas using laser based Bunsen method and kinetic simulation. Fuel, 2012, 95, 206-213.	6.4	73
14	Characteristics of alkali species release from a burning coal/biomass blend. Applied Energy, 2018, 215, 523-531.	10.1	71
15	A review on arsenic removal from coal combustion: Advances, challenges and opportunities. Chemical Engineering Journal, 2021, 414, 128785.	12.7	68
16	Direct Numerical Simulation of Ozone Injection Technology for NOxControl in Flue Gas. Energy & Fuels, 2006, 20, 2432-2438.	5.1	62
17	Ceria substrate–oxide composites as catalyst for highly efficient catalytic oxidation of NO by O 2. Fuel, 2016, 166, 352-360.	6.4	61
18	Catalytic effect of metal chlorides on coal pyrolysis and gasification part I. Combined TG-FTIR study for coal pyrolysis. Thermochimica Acta, 2017, 655, 331-336.	2.7	61

#	Article	IF	CITATIONS
19	Characteristics of O ₃ Oxidation for Simultaneous Desulfurization and Denitration with Limestone–Gypsum Wet Scrubbing: Application in a Carbon Black Drying Kiln Furnace. Energy & Fuels, 2016, 30, 2302-2308.	5.1	59
20	Comparative Investigation on Chlorobenzene Oxidation by Oxygen and Ozone over a MnO _{<i>x</i>} /Al ₂ O ₃ Catalyst in the Presence of SO ₂ . Environmental Science & Technology, 2021, 55, 3341-3351.	10.0	59
21	Effect of Additive Agents on the Simultaneous Absorption of NO ₂ and SO ₂ in the Calcium Sulfite Slurry. Energy & Fuels, 2012, 26, 5583-5589.	5.1	58
22	A review on removal of mercury from flue gas utilizing existing air pollutant control devices (APCDs). Journal of Hazardous Materials, 2022, 427, 128132.	12.4	58
23	Oxy-fuel combustion characteristics and kinetic parameters of lignite coal from thermo-gravimetric data. Thermochimica Acta, 2013, 553, 54-59.	2.7	57
24	Parametrization of the temperature dependence of laminar burning velocity for methane and ethane flames. Fuel, 2019, 239, 1028-1037.	6.4	57
25	New pressurized WSGG model and the effect of pressure on the radiation heat transfer of H2O/CO2 gas mixtures. International Journal of Heat and Mass Transfer, 2018, 121, 999-1010.	4.8	52
26	N ₂ O ₅ Formation Mechanism during the Ozone-Based Low-Temperature Oxidation deNO _{<i>x</i>} Process. Energy & Fuels, 2016, 30, 5101-5107.	5.1	51
27	Review on Magnetic Adsorbents for Removal of Elemental Mercury from Flue Gas. Energy & Fuels, 2020, 34, 13473-13490.	5.1	51
28	Sulfur Transformation during Hydrothermal Dewatering of Low Rank Coal. Energy & Fuels, 2015, 29, 6586-6592.	5.1	50
29	Improving the permittivity of Indonesian lignite with NaCl for the microwave dewatering enhancement of lignite with reduced fractal dimensions. Fuel, 2015, 162, 8-15.	6.4	49
30	A novel photo-thermochemical cycle for the dissociation of CO 2 using solar energy. Applied Energy, 2015, 156, 223-229.	10.1	49
31	Effect of hydrothermal dewatering on the pyrolysis characteristics of Chinese low-rank coals. Applied Thermal Engineering, 2018, 141, 70-78.	6.0	48
32	Laminar burning velocities of CH4/O2/N2 and oxygen-enriched CH4/O2/CO2 flames at elevated pressures measured using the heat flux method. Fuel, 2020, 259, 116152.	6.4	48
33	Effect of preparation method on platinum–ceria catalysts for hydrogen iodide decomposition in sulfur–iodine cycle. International Journal of Hydrogen Energy, 2008, 33, 602-607.	7.1	47
34	Multi-point LIBS measurement and kinetics modeling of sodium release from a burning Zhundong coal particle. Combustion and Flame, 2018, 189, 77-86.	5.2	47
35	Effects of CO content on laminar burning velocity of typical syngas by heat flux method and kinetic modeling. International Journal of Hydrogen Energy, 2014, 39, 9534-9544.	7.1	44
36	Ozone production in parallel multichannel dielectric barrier discharge from oxygen and air: the influence of gas pressure. Journal Physics D: Applied Physics, 2016, 49, 455203.	2.8	43

#	Article	IF	CITATIONS
37	Measurement and kinetics of elemental and atomic potassium release from a burning biomass pellet. Proceedings of the Combustion Institute, 2019, 37, 2681-2688.	3.9	42
38	Direct Numerical Simulation of Subsonic Round Turbulent Jet. Flow, Turbulence and Combustion, 2010, 84, 669-686.	2.6	40
39	Pyrolysis Characteristics and Evolution of Char Structure during Pulverized Coal Pyrolysis in Drop Tube Furnace: Influence of Temperature. Energy & Fuels, 2017, 31, 4799-4807.	5.1	40
40	Catalytic oxidation of NO by O ₂ over CeO ₂ –MnO _x : SO ₂ poisoning mechanism. RSC Advances, 2016, 6, 31422-31430.	3.6	38
41	Measurement of atomic sodium release during pyrolysis and combustion of sodium-enriched Zhundong coal pellet. Combustion and Flame, 2017, 176, 429-438.	5.2	37
42	New weighted-sum-of-gray-gases model for typical pressurized oxy-fuel conditions. International Journal of Energy Research, 2017, 41, 2576-2595.	4.5	36
43	Catalytic effect of metal chlorides on coal pyrolysis and gasification part â¡. Effects of acid washing on coal characteristics. Thermochimica Acta, 2018, 666, 41-50.	2.7	35
44	Quantitative Measurement of Atomic Potassium in Plumes over Burning Solid Fuels Using Infrared-Diode Laser Spectroscopy. Energy & Fuels, 2017, 31, 2831-2837.	5.1	34
45	Enhancement of NO oxidation activity and SO2 resistance over LaMnO3+δ perovskites catalysts with metal substitution and acid treatment. Applied Surface Science, 2019, 479, 234-246.	6.1	34
46	Review on Removal of SO ₂ , NO _{<i>x</i>} , Mercury, and Arsenic from Flue Gas Using Green Oxidation Absorption Technology. Energy & Fuels, 2021, 35, 9775-9794.	5.1	34
47	A novel thermochemical cycle for the dissociation of CO2 and H2O using sustainable energy sources. Applied Energy, 2013, 108, 1-7.	10.1	33
48	A superior liquid phase catalyst for enhanced absorption of NO2 together with SO2 after low temperature ozone oxidation for flue gas treatment. Fuel, 2019, 247, 1-9.	6.4	33
49	Experimental and kinetic modeling study of NO formation in premixed CH4+O2+N2 flames. Combustion and Flame, 2021, 223, 349-360.	5.2	33
50	Efficient degradation of multiple Cl-VOCs by catalytic ozonation over MnO catalysts with different supports. Chemical Engineering Journal, 2022, 435, 134807.	12.7	33
51	Ceria as a catalyst for hydrogen iodide decomposition in sulfur–iodine cycle for hydrogen production. International Journal of Hydrogen Energy, 2009, 34, 1688-1695.	7.1	31
52	Detailed kinetic modeling of homogeneous H2SO4 decomposition in the sulfur–iodine cycle for hydrogen production. Applied Energy, 2014, 130, 396-402.	10.1	31
53	Catalytic decomposition of hydrogen iodide over pre-treated Ni/CeO2 catalysts for hydrogen production in the sulfur–iodine cycle. International Journal of Hydrogen Energy, 2009, 34, 8792-8798.	7.1	28
54	Investigation of NO formation in premixed adiabatic laminar flames of H2/CO syngas and air by saturated laser-induced fluorescence and kinetic modeling. Combustion and Flame, 2016, 164, 283-293.	5.2	28

#	Article	IF	CITATIONS
55	Inhibition of Sodium Release from Zhundong Coal via the Addition of Mineral Additives: Online Combustion Measurement with Laser-Induced Breakdown Spectroscopy (LIBS). Energy & Fuels, 2017, 31, 1082-1090.	5.1	28
56	MnO fabrication with rational design of morphology for enhanced activity in NO oxidation and SO2 resistance. Applied Surface Science, 2020, 503, 144064.	6.1	28
57	Catalytic Thermal Decomposition of Hydrogen Iodide in Sulfurâ^'Iodine Cycle for Hydrogen Production. Energy & Fuels, 2008, 22, 1227-1232.	5.1	27
58	Release characteristic of different classes of sodium during combustion of Zhun-Dong coal investigated by laser-induced breakdown spectroscopy. Science Bulletin, 2015, 60, 1927-1934.	9.0	27
59	Inhibition of sodium release from Zhundong coal via the addition of mineral additives: A combination of online multi-point LIBS and offline experimental measurements. Fuel, 2018, 212, 498-505.	6.4	27
60	Experimental study of potassium release during biomass-pellet combustion and its interaction with inhibitive additives. Fuel, 2020, 260, 116346.	6.4	27
61	A novel double metal ions-double oxidants coactivation system for NO and SO2 simultaneous removal. Chemical Engineering Journal, 2022, 432, 134398.	12.7	27
62	Ozone Production with Dielectric Barrier Discharge from Air: The Influence of Pulse Polarity. Ozone: Science and Engineering, 2018, 40, 494-502.	2.5	26
63	A thermally activated double oxidants advanced oxidation system for gaseous H2S removal: Mechanism and kinetics. Chemical Engineering Journal, 2022, 434, 134430.	12.7	26
64	Electrochemical investigation of the Bunsen reaction in the sulfur–iodine cycle. International Journal of Hydrogen Energy, 2013, 38, 14391-14401.	7.1	25
65	Optimization of microwave dewatering of an Indonesian lignite. Fuel Processing Technology, 2016, 144, 71-78.	7.2	25
66	1.23 Energy and Air Pollution. , 2018, , 909-949.		24
67	Investigation of NO Removal with Ozone Deep Oxidation in Na2CO3 Solution. Energy & Fuels, 2019, 33, 4454-4461.	5.1	24
68	Catalytic decomposition of sulfuric acid over CuO/CeO2 in the sulfur–iodine cycle for hydrogen production. International Journal of Hydrogen Energy, 2015, 40, 2099-2106.	7.1	23
69	Volatile gas release characteristics of three typical Chinese coals under various pyrolysis conditions. Journal of the Energy Institute, 2018, 91, 1045-1056.	5.3	23
70	Investigation of formaldehyde enhancement by ozone addition in CH4/air premixed flames. Combustion and Flame, 2015, 162, 1284-1293.	5.2	22
71	Large-eddy Simulation of Pilot-assisted Pulverized-coal Combustion in a Weakly Turbulent Jet. Flow, Turbulence and Combustion, 2017, 99, 531-550.	2.6	22
72	In Situ Measurements of the Release Characteristics and Catalytic Effects of Different Chemical Forms of Sodium during Combustion of Zhundong Coal. Energy & Fuels, 2018, 32, 6595-6602.	5.1	22

#	Article	IF	CITATIONS
73	Experimental study of Ni/CeO2 catalytic properties and performance for hydrogen production in sulfur–iodine cycle. International Journal of Hydrogen Energy, 2009, 34, 5637-5644.	7.1	21
74	Effect of raw material sources on activated carbon catalytic activity for HI decomposition in the sulfur-iodine thermochemical cycle for hydrogen production. International Journal of Hydrogen Energy, 2016, 41, 7854-7860.	7.1	21
75	Co-precipitation Synthesized MnOx-CeO2 Mixed Oxides for NO Oxidation and Enhanced Resistance to Low Concentration of SO2 by Metal Addition. Catalysts, 2019, 9, 519.	3.5	21
76	Synergistic effect for simultaneously catalytic ozonation of chlorobenzene and NO over MnCoO catalysts: Byproducts formation under practical conditions. Chemical Engineering Journal, 2022, 427, 130929.	12.7	21
77	High-temperature pyrolysis behavior of two different rank coals in fixed-bed and drop tube furnace reactors. Journal of the Energy Institute, 2020, 93, 2271-2279.	5.3	20
78	Interplay effect on simultaneous catalytic oxidation of NO and toluene over different crystal types of MnO2 catalysts. Proceedings of the Combustion Institute, 2021, 38, 5433-5441.	3.9	20
79	Catalytic performance and durability of Ni/AC for HI decomposition in sulfur–iodine thermochemical cycle for hydrogen production. Energy Conversion and Management, 2016, 117, 520-527.	9.2	19
80	Online-CPD-Coupled Large-Eddy Simulation of Pulverized-Coal Pyrolysis in a Hot Turbulent Nitrogen Jet. Combustion Science and Technology, 2017, 189, 103-131.	2.3	19
81	Numerical study of HCl and SO2 impact on potassium emissions in pulverized-biomass combustion. Fuel Processing Technology, 2019, 193, 19-30.	7.2	19
82	Promotional effect of spherical alumina loading with manganese-based bimetallic oxides on nitric-oxide deep oxidation by ozone. Chinese Journal of Catalysis, 2017, 38, 1270-1280.	14.0	18
83	Modelling alkali metal emissions in large-eddy simulation of a preheated pulverised-coal turbulent jet flame using tabulated chemistry. Combustion Theory and Modelling, 2018, 22, 203-236.	1.9	18
84	New oxy-fuel cascade thermo-photovoltaic energy conversion system: Effect of cascade design and oxygen ratio. Energy Conversion and Management, 2019, 196, 1208-1221.	9.2	18
85	High-temperature pyrolysis behavior of a bituminous coal in a drop tube furnace and further characterization of the resultant char. Journal of Analytical and Applied Pyrolysis, 2019, 137, 163-170.	5.5	18
86	Catalytic ozonation of CH2Cl2 over hollow urchin-like MnO2 with regulation of active oxygen by catalyst modification and ozone promotion. Journal of Hazardous Materials, 2022, 436, 129217.	12.4	18
87	Kinetic Modeling of Homogeneous Low-Temperature Multi-Pollutant Oxidation by Ozone. Ozone: Science and Engineering, 2007, 29, 207-214.	2.5	17
88	Effects of Near-Wall Air Application in a Pulverized-Coal 300 MW _e Utility Boiler on Combustion and Corrosive Gases. Energy & Fuels, 2017, 31, 10075-10081.	5.1	17
89	Effect of the Pyrolysis Temperature on the Grindability of Semi-cokes Produced by Two Kinds of Low-Rank Coals. Energy & Fuels, 2018, 32, 1297-1308.	5.1	17
90	Structure and combustion characteristics of semi-cokes from a pilot-scale entrained flow gasifier using oxygen-enriched air. Journal of the Energy Institute, 2021, 97, 80-91.	5.3	17

#	Article	IF	CITATIONS
91	Electrochemical characterization of electrodes in the electrochemical Bunsen reaction of the sulfur–iodine cycle. International Journal of Hydrogen Energy, 2014, 39, 7216-7224.	7.1	16
92	Experimental and numerical study of the effect of elevated pressure on laminar burning velocity of lean H2/CO/O2/diluents flames. Fuel, 2020, 273, 117753.	6.4	16
93	Fully explicit implementation of direct numerical simulation for a transient near-field methane/air diffusion jet flame. Computers and Fluids, 2010, 39, 1381-1389.	2.5	15
94	Thermal efficiency evaluation of a ZnSI thermochemical cycle for CO2 conversion and H2 production – Complete system. International Journal of Hydrogen Energy, 2015, 40, 6004-6012.	7.1	15
95	SO3 decomposition over CuO–CeO2 based catalysts in the sulfur–iodine cycle for hydrogen production. International Journal of Hydrogen Energy, 2018, 43, 14876-14884.	7.1	15
96	Effects of gas preheat temperature on soot formation in co-flow methane and ethylene diffusion flames. Proceedings of the Combustion Institute, 2021, 38, 1225-1232.	3.9	15
97	Premixed jet flame characteristics of syngas using OH planar laser induced fluorescence. Science Bulletin, 2011, 56, 2862-2868.	1.7	13
98	HI Decomposition over Carbon-Based and Ni-Impregnated Catalysts of the Sulfur–lodine Cycle for Hydrogen Production. Industrial & Engineering Chemistry Research, 2015, 54, 1498-1504.	3.7	13
99	Physicochemical properties of wastewater produced from the microwave upgrading process of Indonesian lignite. Fuel, 2015, 158, 435-442.	6.4	13
100	The effects of gas flow pattern on the generation of ozone in surface dielectric barrier discharge. Plasma Science and Technology, 2019, 21, 055505.	1.5	13
101	High-Performance Pt Catalyst with Graphene/Carbon Black as a Hybrid Support for SO ₂ Electrocatalytic Oxidation. Langmuir, 2020, 36, 20-27.	3.5	13
102	Combustion and NO _{<i>x</i>} Emission Characteristics with Respect to Staged-Air Damper Opening in a 600 MW _e Down-Fired Pulverized-Coal Furnace under Deep-Air-Staging Conditions. Environmental Science & Technology, 2014, 48, 837-844.	10.0	12
103	Catalytic Effect of Metal Chloride Additives on the Volatile Gas Release Characteristics for High-Temperature Lignite Pyrolysis. Energy & Fuels, 2019, 33, 9437-9445.	5.1	12
104	Numerical study of HCl and SO2 impact on sodium emissions in pulverized-coal flames. Fuel, 2019, 250, 315-326.	6.4	12
105	The interaction between microwave and coal: A discussion on the state-of-the-art. Fuel, 2022, 314, 123140.	6.4	12
106	The Influence of Anionic Additives on the Microwave Dehydration Process of Lignite. Energy & Fuels, 2020, 34, 9401-9410.	5.1	11
107	A novel flame energy grading conversion system: Preliminary experiment and thermodynamic parametric analysis. International Journal of Energy Research, 2020, 44, 2084-2099.	4.5	11
108	Effects of the Gas Preheat Temperature and Nitrogen Dilution on Soot Formation in Co-flow Methane, Ethane, and Propane Diffusion Flames. Energy & Fuels, 2021, 35, 7169-7178.	5.1	11

#	Article	IF	CITATIONS
109	Catalytic Decomposition of Residual Ozone over Cactus-like MnO ₂ Nanosphere: Synergistic Mechanism and SO ₂ /H ₂ O Interference. ACS Omega, 2022, 7, 9818-9833.	3.5	11
110	Enhancement of lignite microwave dehydration by cationic additives. Fuel, 2021, 289, 119985.	6.4	10
111	Characteristics and evolution of products under moderate and high temperature coal pyrolysis in drop tube furnace. Journal of the Energy Institute, 2021, 96, 121-127.	5.3	10
112	Direct numerical simulation of hydrogen turbulent lifted jet flame in a vitiated coflow. Science Bulletin, 2007, 52, 2147-2156.	1.7	9
113	Effects of CH ₄ Content on NO Formation in One-Dimensional Adiabatic Flames Investigated by Saturated Laser-Induced Fluorescence and CHEMKIN Modeling. Energy & Fuels, 2017, 31, 3154-3163.	5.1	9
114	NO _{<i>x</i>} Reduction in a 130 t/h Biomass-Fired Circulating Fluid Bed Boiler Using Coupled Ozonation and Wet Absorption Technology. Industrial & Engineering Chemistry Research, 2019, 58, 18134-18140.	3.7	9
115	Effects of Nafion content in membrane electrode assembly on electrochemical Bunsen reaction in high electrolyte acidity. International Journal of Hydrogen Energy, 2019, 44, 11646-11654.	7.1	9
116	Dynamic zinc and potassium release from a burning hyperaccumulator pellet and their interactions with inhibitive additives. Fuel, 2021, 286, 119365.	6.4	9
117	Equilibrium potential for the electrochemical Bunsen reaction in the sulfur–iodine cycle. International Journal of Hydrogen Energy, 2014, 39, 18727-18733.	7.1	8
118	Study on CuO-CeO ₂ /SiC catalysts in the sulfur-iodine cycle for hydrogen production. International Journal of Energy Research, 2016, 40, 1062-1072.	4.5	8
119	Influences of Hydrothermal Modification on Nitrogen Thermal Conversion of Low-Rank Coals. Energy & Fuels, 2016, 30, 8125-8133.	5.1	8
120	Catalyst tolerance to SO ₂ and water vapor of Mn based bimetallic oxides for NO deep oxidation by ozone. RSC Advances, 2017, 7, 25132-25143.	3.6	8
121	Ignition, puffing and sooting characteristics of kerosene droplet combustion under sub-atmospheric pressure. Fuel, 2021, 285, 119182.	6.4	8
122	Promotion effect of activated carbon, coal char and graphite on lignite microwave dehydration process. Journal of Analytical and Applied Pyrolysis, 2022, 161, 105380.	5.5	8
123	Effects of the Equivalence Ratio and Reynolds Number on Turbulence and Flame Front Interactions by Direct Numerical Simulation. Energy & Fuels, 2016, 30, 6727-6737.	5.1	7
124	Study of the mechanism of the catalytic decomposition of hydrogen iodide (HI) over carbon materials for hydrogen production. International Journal of Hydrogen Energy, 2017, 42, 4977-4986.	7.1	7
125	Ozone Production Influenced by Increasing Gas Pressure in Multichannel Dielectric Barrier Discharge for Positive and Negative Pulse Modes. Ozone: Science and Engineering, 2018, 40, 228-236.	2.5	7
126	Reaction Mechanism Reduction for Ozone-Enhanced CH4/Air Combustion by a Combination of Directed Relation Graph with Error Propagation, Sensitivity Analysis and Quasi-Steady State Assumption. Energies, 2018, 11, 1470.	3.1	7

#	Article	IF	CITATIONS
127	Interactive Effects in Two-Droplets Combustion of RP-3 Kerosene under Sub-Atmospheric Pressure. Processes, 2021, 9, 1229.	2.8	7
128	The Benefits of Small Quantities of Nitrogen in the Oxygen Feed to Ozone Generators. Ozone: Science and Engineering, 2018, 40, 313-320.	2.5	6
129	H2SO4 poisoning of Ru-based and Ni-based catalysts for HI decomposition in Sulfur Iodine cycle for hydrogen production. International Journal of Hydrogen Energy, 2019, 44, 9771-9778.	7.1	6
130	SO ₂ Electrocatalytic Oxidation Properties of Pt–Ru/C Bimetallic Catalysts with Different Nanostructures. Langmuir, 2020, 36, 3111-3118.	3.5	5
131	Simulation and Economic Research of Circulating Cooling Water Waste Heat and Water Resource Recovery System. Energies, 2021, 14, 2496.	3.1	5
132	Effects of CO ₂ Dilution and CH ₄ Addition on Laminar Burning Velocities of Syngas at Elevated Pressures: An Experimental and Modeling Study. Energy & Fuels, 2021, 35, 18733-18745.	5.1	5
133	<scp>LCA</scp> comparison analysis for two types of <scp> H ₂ </scp> carriers: Methanol and ammonia. International Journal of Energy Research, 2022, 46, 11818-11833.	4.5	5
134	Metal chloride influence on syngas component during coal pyrolysis in fixed-bed and entrained flow drop-tube furnace. Science China Technological Sciences, 2019, 62, 2029-2037.	4.0	4
135	Kinetics and Mechanisms of Metal Chlorides Catalysis for Coal Char Gasification with CO2. Catalysts, 2020, 10, 715.	3.5	4
136	Investigation of Hydrogen Content and Dilution Effect on Syngas/Air Premixed Turbulent Flame Using OH Planar Laser-Induced Fluorescence. Processes, 2021, 9, 1894.	2.8	4
137	Decomposition of N ₂ 0 on ZIF-67-Derived Co/CoO _{<i>x</i>} @Carbon Catalysts and SO ₂ Interference. Energy & Fuels, 2021, 35, 18664-18679.	5.1	4
138	United Conversion Process Coupling CO ₂ Mineralization with Thermochemical Hydrogen Production. Environmental Science & amp; Technology, 2019, 53, 12091-12100.	10.0	3
139	A projection procedure to obtain adiabatic flames from non-adiabatic flames using heat flux method. Proceedings of the Combustion Institute, 2021, 38, 2143-2151.	3.9	3
140	Development of reduced and optimized reaction mechanism for potassium emissions during biomass combustion based on genetic algorithms. Energy, 2020, 211, 118565.	8.8	3
141	Verification and Validation of a Low-Mach-Number Large-Eddy Simulation Code against Manufactured Solutions and Experimental Results. Energies, 2018, 11, 921.	3.1	2
142	Effect of carbonization temperature on the grindability of carbonaceous material produced from different coals. Canadian Journal of Chemical Engineering, 2019, 97, 2653-2661.	1.7	2
143	Impact of Pyrolysis Products on <i>n</i> -Decane Laminar Flame Speeds Investigated through Experimentation and Kinetic Simulations. Energy & Fuels, 2021, 35, 8194-8204.	5.1	2
144	Comparative Study of Four Chemometric Methods for the Quantitative Analysis of the Carbon Content in Coal by Laser-Induced Breakdown Spectroscopy Technology. ACS Omega, 2022, 7, 9443-9451.	3.5	2

#	Article	IF	CITATIONS
145	Pyrolysis characteristics of lowâ€rank coals based on doubleâ€gaussian distributed activation energy model. Canadian Journal of Chemical Engineering, 2019, 97, 2642-2652.	1.7	1
146	Reduced chemical reaction mechanisms for simulating sodium emissions by solid-fuel combustion. Applications in Energy and Combustion Science, 2020, 1-4, 100009.	1.5	1
147	Investigation of Dilution Effect on CH4/Air Premixed Turbulent Flame Using OH and CH2O Planar Laser-Induced Fluorescence. Energies, 2020, 13, 325.	3.1	1
148	ICOPE-15-C133 DNS Investigation of the Interaction between Premixed Turbulent Syngas Flame Front and Vortex at Different Reynolds Numbers. The Proceedings of the International Conference on Power Engineering (ICOPE), 2015, 2015.12, _ICOPE-15ICOPE-15	0.0	0
149	Catalytic and Sulfur-Tolerant Performance of Bimetallic Ni–Ru Catalysts on HI Decomposition in the Sulfur-Iodine Cycle for Hydrogen Production. Energies, 2021, 14, 8539.	3.1	Ο
150	Three-Dimensional Direct Numerical Simulation of Near-Field Ozone-Enhanced Lean Premixed Syngas Turbulent Jet Flame. Energies, 2022, 15, 3945.	3.1	0